WATER RESOURCES RESEARCH, VOL. 37, NO. 1, PAGES 21–31, JANUARY 2001

A new tracer-density criterion for heterogeneous porous media

Gilbert R. Barth,[1,2] Tissa H. Illangasekare,[3] Mary C. Hill,[2] and Harihar Rajaram[1]

Abstract. Tracer experiments provide information about aquifer material properties vital for accurate site characterization. Unfortunately, density-induced sinking can distort tracer movement, leading to an inaccurate assessment of material properties. Yet existing criteria for selecting appropriate tracer concentrations are based on analysis of homogeneous media instead of media with heterogeneities typical of field sites. This work introduces a hydraulic-gradient correction for heterogeneous media and applies it to a criterion previously used to indicate density-induced instabilities in homogeneous media. The modified criterion was tested using a series of two-dimensional heterogeneous intermediate-scale tracer experiments and data from several detailed field tracer tests. The intermediate-scale experimental facility ($10.0 \times 1.2 \times 0.06$ m) included both homogeneous and heterogeneous ($\sigma^2_{\ln k} = 1.22$) zones. The field tracer tests were less heterogeneous ($0.24 < \sigma^2_{\ln k} < 0.37$), but measurements were sufficient to detect density-induced sinking. Evaluation of the modified criterion using the experiments and field tests demonstrates that the new criterion appears to account for the change in density-induced sinking due to heterogeneity. The criterion demonstrates the importance of accounting for heterogeneity to predict density-induced sinking and differences in the onset of density-induced sinking in two- and three-dimensional systems.

1. Introduction

Determining appropriate values of constitutive parameters for groundwater systems, such as hydraulic conductivity and dispersivity, is critical for site characterization, numerical modeling, and development of remediation scenarios. Heterogeneity and limitations of discrete, field-site sampling constrain our ability to characterize the subsurface. Tracer tests provide one of the few ways to obtain an integrated response of the system at an appropriate scale. Many researchers commonly use tracer tests to determine parameter values such as hydraulic conductivity and dispersivity [*Jensen et al*., 1993; *Adams and Gelhar*, 1992; *Garabedian et al*., 1991; *Moltyaner and Wills*, 1991; *Freyberg*, 1986; *Sudicky*, 1986].

The interpretation of conservative tracer tests typically assumes that the tracer moves with the groundwater so that the tracer's spatial and temporal distribution reflects the distribution of subsurface material properties pertinent to the movement of groundwater. Ensuring this requires a tracer that is similar to the ambient groundwater in terms of both physicochemical interaction with the porous media and density. Similar physicochemical interaction ensures that the tracer progress is neither attenuated nor retarded relative to the ambient groundwater. Similar density ensures that transport driven by a hydraulic gradient (forced convection) determines transport and that density-induced sinking is insignificant.

Observations and analysis of leachate plume sinking from previously published experiments [e.g., *Oostrom et al*., 1992a, 1992b; *Schincariol and Schwartz*, 1990; *List*, 1965] provide insight into the density-induced sinking of tracer plumes. This paper builds on the analysis of *Oostrom et al*. [1992a], which presented a criterion for the propensity of a dense tracer plume to exhibit density-induced instabilities, and presents a criterion for creating a tracer plume free of density-induced sinking. The specific mechanism of sinking is not the focus of this paper, only the tendency for sinking to occur and its relation to the density contrast between tracer plume and ambient groundwater. It is hypothesized that the relationship between density-induced instabilities in a dense tracer plume and the propensity for the dense plume to sink can be used to evaluate density-induced sinking in general. This is expected to be valid because the onset of instabilities in experiments by *Oostrom et al*. [1992a, 1992b], *Schincariol and Schwartz* [1990], and *List* [1965] was coincident with the detection of density-induced sinking. Differences in the mechanics of sinking between two- and three-dimensional systems, such as whether the onset of density-induced sinking is predominantly in the longitudinal or transverse directions [e.g., *Liu and Dane*, 1997; *Liu*, 1995], are not addressed. The criterion is not intended to discriminate between such differences but to serve only as a simple indicator of the potential for density-induced sinking.

This work presents a hydraulic-gradient correction for heterogeneous media and applies it to *Oostrom et al*.'s [1992a] original criterion, which was tested in homogeneous media, to produce a new criterion for the assessment of density-induced tracer plume sinking in heterogeneous media. This new criterion is then tested using intermediate-scale experimental results and data from several field sites. The hydraulic-gradient correction could be also be applied to any criterion that includes or can be rearranged to include hydraulic gradient.

This paper begins by reviewing published field and laboratory experiments and derives a hydraulic-gradient correction for heterogeneous media. The hydraulic-gradient correction is incorporated into a new criterion for predicting density-induced sinking in heterogeneous media. Details of a series of

[1]Department of Civil and Environmental Engineering, University of Colorado, Boulder.
[2]U.S. Geological Survey, Boulder, Colorado.
[3]Division of Environmental Sciences and Engineering, Colorado School of Mines, Golden.

Paper number 2000WR900287.
0043-1397/01/2000WR900287$09.00

intermediate-scale experiments and brief descriptions of previously published field tracer tests are then presented. Data from these experiments are used to evaluate the performance of the new criterion. Finally, the importance of the hydraulic-gradient correction is evaluated with respect to system dimensionality, heterogeneity, and large-scale gradients.

1.1. Field Experiments

Producing a tracer plume that reflects subsurface heterogeneity requires careful consideration of several factors, including preparation of the tracer solution and the method of delivery into the subsurface. The tracer is usually prepared by mixing a concentrated form with local groundwater that has been extracted from the aquifer. Use of local groundwater eliminates many of the potential physicochemical and density contrasts between the injected tracer and the ambient groundwater. In most cases, however, the addition of tracer concentrate to the extracted groundwater results in a tracer solution of greater density than the ambient groundwater. Typically, the tracer is injected over a short period to produce a well-defined region of uniform concentration that is surrounded by the ambient groundwater and of sufficient concentration to be detected at the sampling locations. Creation of such a well-defined source over a short time period simplifies both simulation and analysis of the tracer transport. In addition, an injection of extended duration is susceptible to changing physical conditions. For example, cooling of the tracer reservoir by changes in air temperature, while the subsurface temperature remains relatively stable, would increase the relative density of the injected tracer.

Detection of density-induced sinking requires detailed observations that often are unavailable. The variability of subsurface properties and their impact on transport [e.g., *Boggs et al*., 1992] can easily mask the occurrence of a sinking plume. Well-documented tracer tests conducted at the Borden Air Force Base in Canada [*Freyberg*, 1986; *Mackay et al*., 1986], the Otis Air Force Base at Cape Cod in the United States [*Garabedian et al*., 1991; *LeBlanc et al*., 1991], and the Jutland Peninsula in Denmark [*Jensen et al*., 1993] are examples of the few field experiments with sufficiently detailed data on subsurface heterogeneity that density-induced sinking can be identified as the cause of a tracer plume's vertical migration. These experiments used a variety of reactive (e.g., lithium, fluoride, carbon tetrachloride) and nonreactive (e.g., chloride, bromide, tritium) tracers and a large number of samplers to capture the spatial distribution of the solute plume as it evolved with time. Because of the extensive sampling arrays, it was apparent that despite attempts to create an ideal ambient-density tracer plume, experiments at each of the sites experienced density-induced sinking [*Jensen et al*., 1993; *LeBlanc and Celia*, 1991; *Freyberg*, 1986]. Considering the elaborate and detailed nature of these experiments, it seems probable that density-induced sinking goes undetected in many tracer tests. The only way to prevent density-induced sinking, and the bias it introduces to experimental results, is to develop guidelines so that tracer-test configurations susceptible to density-induced sinking can be avoided.

1.2. Laboratory Experiments

A number of laboratory experiments have been conducted to investigate the effects of density contrasts on flow in porous media. Experiments by *Istok and Humphrey* [1995] demonstrated the influence of contrasts in tracer and ambient groundwater density on the evaluation of dispersivity. They used a 4-m-long, 2-m-wide, and 20-cm-deep tank with homogeneous packing, doublet well system, and constant-head boundaries on each end [*Humphrey*, 1992]. The tracer was injected over the entire interval of a fully penetrating well, creating a scenario similar to saltwater intrusion, where the denser fluid forces the lighter fluid ahead and creates a sloped interface reflecting the contrast between the tracer density (ρ_s) and the ambient solution density (ρ_0). Relative densities ($\rho_{rel} = (\rho_s - \rho_0)/\rho_0$), ranging from 0.000074 to 0.0015, were evaluated. The results demonstrated a significant increase in calculated dispersivity as a function of increasing tracer concentration. For this particular experimental configuration, effects of density contrasts were found down to very low ρ_{rel}. Although their experiment was one of the few to specifically address density contrasts during tracer tests, Istok and Humphrey did not evaluate the behavior of a dense miscible plume overlying a less dense solution, a situation common in tracer tests.

Much of the experimental work examining the dynamics of a denser miscible fluid overlying a less dense one has focused on hydrodynamic instabilities [e.g., *Wooding*, 1959, 1962, 1969; *List*, 1965; *Bachmat and Elrick*, 1970; *Libicki*, 1978; *Paschke and Hoopes*, 1984; *Schincariol and Schwartz*, 1990; *Oostrom et al*., 1992a, 1992b]. Although these investigations were not specifically focused on tracers, their assessment of hydrodynamic instabilities and the resulting potential for density-induced sinking can be applied to tracers. The distinction between stable and unstable flow is defined as the critical point at which differences in density may disturb the mechanical equilibrium by inducing free convection currents [*Bachmat and Elrick*, 1970]. Instabilities are evident by lobe-shaped protuberances that form first along the bottom edge of the plume and later within the plume [*Schincariol and Schwartz*, 1990]. Most of the work was performed in homogeneous materials. Experiments by *Wooding* [1959, 1962, 1969] were used to study the instability of interfaces between two fluids of different densities initially at rest. Displacement in both column experiments [*Wooding*, 1959, 1962] and Hele-Shaw experiments [*Wooding*, 1969] occurred as a series of viscous fingers, reflecting the instability of the interface between the two solutions of different densities. *List* [1965], *Libicki* [1978], *Paschke and Hoopes* [1984], *Schincariol and Schwartz* [1990], and *Oostrom et al*. [1992a, 1992b] examined the potential for density-induced sinking in forced convection systems with a range of ρ_{rel}. Analysis and experiments by *List* [1965] indicated that the fluid boundary was unstable for all situations but the growth rates of instability could be so low as to result in quasi-stable flow, in which the minor instabilities at the interface between the ambient fluid and overlying denser solution tend to dampen out, resulting in no significant sinking of the plume centroid. Using plumes with $\rho_{rel} \approx 0.027$, *Libicki* [1978] demonstrated that saturated hydraulic conductivity and the velocity of the ambient groundwater were significant factors influencing the shape of contaminant plumes. *Paschke and Hoopes* [1984] focused on the trajectory of the plume as a function of ρ_{rel}. *Schincariol and Schwartz* [1990] introduced plumes with a range of ρ_{rel} into both homogeneous and simple heterogeneous systems. Their work demonstrated a wide range of transport behavior, from $\rho_{rel} = 0.0001$ without any density-induced sinking to $\rho_{rel} = 0.0681$ with considerable density-induced sinking. Work by *Oostrom et al*. [1992a] included a similar range of ρ_{rel} ($0.0001 < \rho_{rel} < 0.0360$) in two different homogeneous media and several

different tanks. Using a gamma radiation system, *Oostrom et al*. [1992b] quantitatively mapped instabilities due to differences in density of the ambient groundwater and the solute plume.

1.3. Dimensionless Criteria

The tendency for a density contrast to result in sinking is offset by forced convection, diffusion, and viscosity. Many of the cited laboratory investigations used a dimensionless ratio to quantify this relationship. For example, *Wooding* [1959] developed a criterion based on the Rayleigh number that incorporated vertical density gradient, gravity, permeability, column radius, mean viscosity of the two fluids, and apparent diffusivity of the medium. Systems that exceeded the critical value would be unstable.

Oostrom et al. [1992a] presented several criteria for predicting onset of instabilities in laboratory experiments involving forced convection. The criteria compare factors in a flowing system that contribute to the stability of the interface between dense solute plumes overlying less dense fluids with the factors contributing to instabilities. The first, a relatively simple ratio, did not incorporate terms specifically related to plume shape [*Oostrom et al*., 1992a, equation (3)]:

$$\alpha_1 = \frac{\left(K\,\dfrac{\Delta\rho}{\rho}\right)}{q}, \tag{1}$$

where, for isotropic materials, K is saturated hydraulic conductivity $[L/T]$, $\Delta\rho$ is solute density minus ambient groundwater density $[M/L^3]$, ρ is ambient groundwater density $[M/L^3]$, and q is the magnitude of the Darcy flux $[L/T]$. The second ratio was a modified Rayleigh number [*Oostrom et al*., 1992a, equation (4)], but Oostrom's analysis indicates that (1) provides a more consistent indicator for the onset of instabilities. On the basis of their own results and using data from *List* [1965] and *Schincariol and Schwartz* [1990], *Oostrom et al*. [1992a] determined that plumes with a value of $\alpha_1 > 0.3$ were unstable while those with $\alpha_1 < 0.3$ appeared to be unaffected by the contrast in density. Thus 0.3 is a critical value of α_1. This criterion and the critical value depend only on the flow field and density contrasts experienced within the porous media. The critical value was consistent across the variety of materials, source configurations, and boundary conditions used in all the experiments.

List's [1965] results, indicating that a dense plume above a lighter fluid is inherently unstable, suggest that the critical value observed for (1) does not distinguish between stable and unstable, but between quasi-stable and unstable. Experiments performed by *List* [1965], *Schincariol and Schwartz* [1990], and *Oostrom et al*. [1992a, 1992b], in which a dense plume overlying a less dense solution does not sink over the length of the experiment, are, according to List's analysis, quasi-stable. For plumes for which (1) is less than 0.3 the experimental results did not indicate any significant density-induced sinking [e.g., *List*, 1965; *Schincariol and Schwartz*, 1990; *Oostrom et al*., 1992a, 1992b]. Exceeding the critical value of (1) should be interpreted as an indication of density contrasts sufficient to result in significant density-induced sinking.

Exceeding the critical value of α_1 can produce a variety of plume characteristics but will consistently result in significant density-induced sinking. For example, the lobe-shaped protuberances typically defined as instabilities are not evident in some of the denser plumes created by *Schincariol and Schwartz* [1990, e.g., Figure 6], even though the plume is clearly sinking due to hydrodynamic instabilities. Capturing the direct evidence of hydrodynamic instabilities requires very specialized experiments, but there is considerable evidence to support the correspondence between exceeding the critical value of $\alpha_1 = 0.3$ and the existence of density-induced sinking for dense miscible plumes overlying less dense liquids [e.g., *List*, 1965; *Schincariol and Schwartz*, 1990; *Oostrom et al*., 1992a, 1992b].

1.4. Numerical Simulations

A number of investigators have performed simulations of density-induced sinking for plumes with relatively low density contrasts [e.g., *Oostrom et al*., 1992c; *Fan and Kahawita*, 1994; *Schincariol et al*., 1994; *Liu and Dane*, 1997]. All these simulations relied on an additional term or truncation and round-off errors to create the small perturbations that produced hydrodynamic instabilities and the resultant density-induced sinking. The simulations were able to qualitatively reproduce the density-induced sinking observed in physical experiments. Because the results depend, however, on adjusting or dampening the small perturbations, the simulations do not provide a mechanism for investigating the critical conditions at which tracer plumes transition from the state of no significant density-induced sinking to that of significant density-induced sinking.

2. Development of Criteria for Heterogeneous Systems

In its current form, the criterion given as (1) is limited to homogeneous situations. Heterogeneity can create conditions in which it is possible to have local flows that are orders of magnitude smaller than the average flow rate, providing significant opportunity for sinking not indicated by the average flow rate. For field sites where the local flow rates vary over orders of magnitude, α_1 considerably underestimates the potential for sinking. Thus for systems with more than mild heterogeneity the definition of α_1 should be modified to account for variable flow.

For the analysis of heterogeneous systems, (1) is first rewritten in a more convenient form by using Darcy's law to substitute $q/K = |\Delta h/\Delta l|$, where $\Delta h/\Delta l$ is the hydraulic gradient. Substituting also $\rho_{\text{rel}} = \Delta\rho/\rho$ produces

$$\alpha_1' = \frac{(\rho_{\text{rel}})}{\left|\dfrac{\Delta h}{\Delta l}\right|}. \tag{2}$$

It is hypothesized that this equation can be applied locally in homogeneous lenses of a heterogeneous porous media to detect the potential for density-induced sinking. Equation (2) inherently assumes that within individual lenses, K is constant and isotropic. In words, α_1' is the ratio of the relative density difference to the hydraulic gradient. From this perspective, for a given concentration difference, the magnitude of the hydraulic gradient must stay above a critical value to produce a plume free of density-induced sinking.

Application of (2) to each lens in a heterogeneous system would be impractical. A modification to α_1', which accounts for the variability of the local gradient in heterogeneous systems, is needed to produce an appropriate dimensionless parameter. The statistics of the local gradient, based on the distribution of hydraulic conductivity and the overall gradient, can provide a range of probable gradients for the system. Using the low end

of this range instead of the overall gradient more accurately reflects the opportunity for density-induced sinking to occur during a tracer test.

The first step in modifying α_1' is to obtain an expression for the variability of the local gradient. This is accomplished by using a statistical characterization of K and producing an equation for the variation in local gradient (j_i) as a function of the statistics of K. Applying basic principles of stochastic analysis [see, e.g., *Gelhar*, 1993, chapter 4], the head perturbation expression is

$$\frac{\partial^2 h}{\partial x_i^2} - \frac{\partial f}{\partial x_i} J_i = 0, \tag{3}$$

where h is head, J_i represents the overall gradient, and f is the perturbation of ln K. This form assumes that there is no trend in the mean log hydraulic conductivity. For this work it is assumed that the principal flow direction is aligned with the first coordinate direction. Using spectral representations of h and f in (3) gives

$$\frac{\partial^2}{\partial x_i^2}\left(\int_{-\infty}^{\infty}\int_{-\infty}^{\infty} e^{ik_i x_i}\, dZ_h(\vec{k})\right) - J_i \frac{\partial}{\partial x_i}\left(\int_{-\infty}^{\infty}\int_{-\infty}^{\infty} e^{ik_i x_i}\, dZ_f(\vec{k})\right) = 0, \tag{4}$$

where $dZ_h(\vec{k})$ is the spectral amplitude of the head, $dZ_f(\vec{k})$ is the spectral amplitude of the ln K perturbations, and k_i is the wavenumber in the ith coordinate direction. Solving for the head spectral amplitude, differentiating with respect to x, and multiplying by its complex conjugate produces for a two-dimensional system an expression for $\sigma_{j_1}^2$, the variance of j_1:

$$\sigma_{j_1}^2 = \frac{\sigma_f^2 J_1^2}{\pi} \int_0^{2\pi} \frac{\cos^4\theta}{(\cos^2\theta + r^2 \sin^2\theta)^2}\, d\theta, \tag{5}$$

where $r^2 = (\lambda_l/\lambda_t)^2$, λ_l and λ_t are the longitudinal and transverse correlation scales, respectively, and the negative exponential function was used to represent the covariance of the random ln K field. Similar manipulations for the three-dimensional case produce an equivalent expression for three dimensions:

$$\sigma_{j_1}^2 = \frac{\sigma_f^2 J_1^2}{4\pi} \cdot \int_1^{-1}\int_0^{2\pi} \frac{-u^4}{(u^2 + (1-u^2)(\sin^2\theta + r^2\cos^2\theta))^2}\, d\theta\, du. \tag{6}$$

For the three-dimensional case, $r = \lambda_l/\lambda_v$, λ_v is the vertical correlation scale, and it is assumed that $\lambda_l = \lambda_t$; that is, the correlation structure is assumed to be isotropic in the horizontal plane. Numerically integrating (5) for a two-dimensional flow field or (6) for a three-dimensional flow field provides a value for $\sigma_{j_1}^2$, which can then be used to define a range within which the overall gradient is likely to occur as

$$J - 2\sigma_{j_1} < J < J + 2\sigma_{j_1}. \tag{7}$$

Finally, the lower limit of the range in (7) is used to replace the overall gradient term in α_1' to produce

$$\alpha_2 = \frac{(\rho_{\text{rel}})}{(J - 2\sigma_{j_1})}. \tag{8}$$

If the distribution of local gradients is approximately Gaussian, a reasonable approximation for mild heterogeneity, then the denominator represents the lower end of the local-gradient 95% confidence interval. As the degree of heterogeneity increases, this interpretation of the denominator becomes less reasonable. Considering the degree of heterogeneity evaluated in this paper ($\sigma_{\ln k}^2 \leq 1.22$), the Gaussian interpretation was used. It is hypothesized that α_2 is capable of predicting density-induced sinking in heterogeneous porous media using a critical value of 0.3. The value of α_2 is a conservative measure because the low end of the hydraulic gradient values is used for evaluation.

A simple rearrangement of (8), using the critical value of $\alpha_2 = 0.3$, provides an expression for the maximum tracer density for a given system based on the variability of hydraulic conductivity, overall gradient at the site, and the density of ambient groundwater:

$$\rho_s < \rho_0 + \rho_0 0.3(J - 2\sigma_{j_1}). \tag{9}$$

Equation (9) indicates that the density difference between the tracer and adjacent groundwater must be less than a factor of $0.3(J - \sigma_{j_1}^2)$, which, considering typical field gradients, may be very small. For extremely heterogeneous systems, it is possible for the second term on the right-hand side of (9) to be negative. The resulting suggestion that ρ_s would need to be less than ρ_0 is, of course, invalid.

In this work, ρ_s is taken to be at the injected concentration, C_0. Immediately following injection, portions of a plume can experience significant dilution, decreasing the potential for density-induced sinking. In many cases, however, and as will be shown for the situations considered in this work, a sufficient volume is injected so that the injected plume displaces the ambient groundwater and concentrations at the centroid decrease slowly. For any tracer test, as the plume becomes diluted to concentrations much lower than C_0, evaluation of a dimensionless criterion to determine the potential for density-induced sinking should be based on an estimate of solute concentrations, which could be based on numerical simulations or actual observations.

3. Testing the Criteria for Heterogeneous Systems

Evaluation of the viability of (8) would ideally be accomplished using data from field experiments spanning a range of heterogeneity. As discussed previously, however, there are only a limited number of field tracer tests with sufficiently detailed measurements and observations. In addition, typical gradients imposed during forced gradient tests are large enough to virtually eliminate the issue of density-induced sinking [e.g., *Yeh et al*., 1995], and interpretation of data from sites where the material properties are not second-order stationary [e.g., *Boggs et al*., 1992] is problematic. Equation (8) is therefore evaluated using data from several field sites with relatively mild heterogeneity [*Freyberg*, 1986; *Mackay et al*., 1986; *Garabedian et al*., 1991; *LeBlanc et al*., 1991; *Jensen et al*., 1993] and a series of more heterogeneous, but still second-order stationary, intermediate-scale laboratory experiments conducted as part of this work.

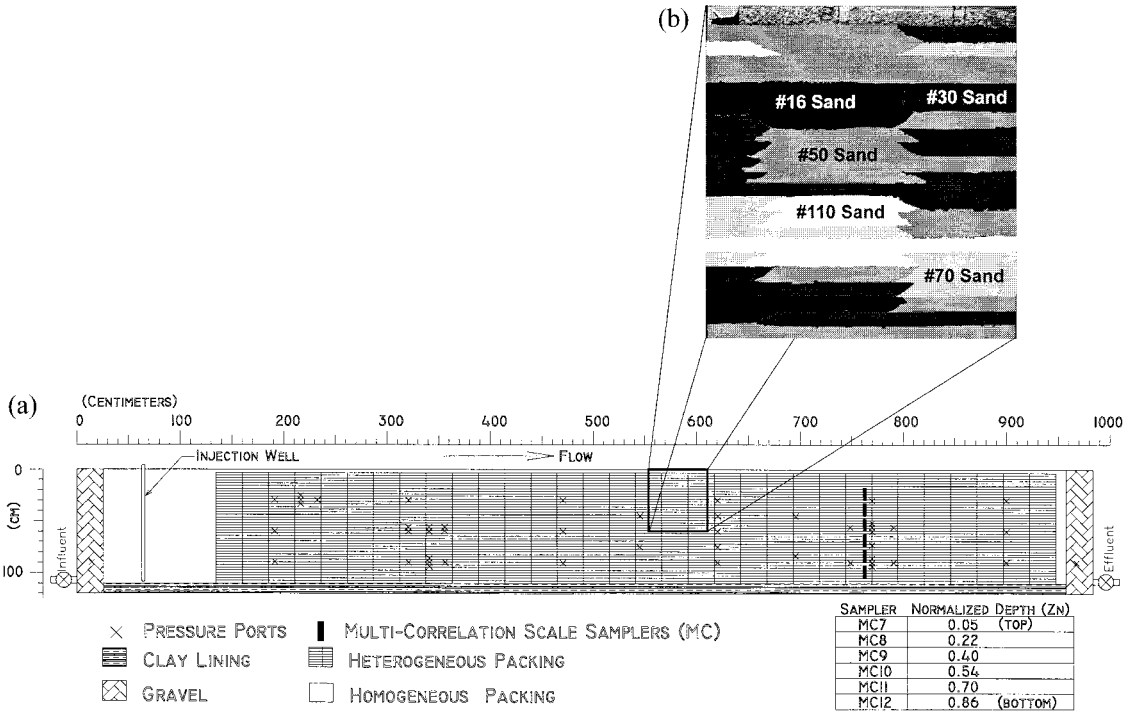

Figure 1. (a) Intermediate-scale tank for solute transport experiments in heterogeneous porous media. Pressure ports, injection well, and samplers are indicated. (b) Enhanced gray scale detail of the tank packing. Five sands are in a random distribution. Image is of section ~1/2 the tank height and 1/16th of the length. Each lens is 25.4 cm long and 2.54 cm tall and is tapered at the ends.

In the past, even the more complicated laboratory studies mentioned above [e.g., *Schincariol and Schwartz*, 1990] focused on relatively simple heterogeneous systems. Statistics of such porous media packings could not be compared with natural, heterogeneous field systems, thereby limiting interpretation of the results. In this work, intermediate-scale tracer test experiments were performed in a 10-m-long, two-dimensional porous-media tank. The size of the tank and complexity of the porous medium packing provided a controlled, completely defined system of multiple correlation lengths, large enough to have statistical properties resembling field sites. The degree of heterogeneity of the intermediate-scale experiment was designed to be considerably more than that observed at Borden [*Freyberg*, 1986; *Mackay et al*., 1986], Cape Cod [*Garabedian et al*., 1991; *LeBlanc et al*., 1991], and the Danish site [*Jensen et al*., 1993]. The following sections describe the experiments in some detail.

4. Intermediate-Scale Experiments

4.1. Design and Construction

A series of six intermediate-scale tracer tests were performed. Three of the tests exemplify the results and are highlighted in this paper. The tracer injection and sampling were executed in accordance with the ideal conservative tracer discussed above: Injection occurred over as brief an interval as practical, and the sample size and frequency were limited to minimize the impact on the flow field. The first five tests used bromide as a tracer and produced a series of breakthrough curves (BTCs) for transport mechanisms ranging from a mixture of density-induced sinking and forced convection to forced convection alone, depending on the tracer concentration. The sixth test, conducted using tritium as a tracer and therefore subject only to forced convection, served as a control.

4.2. Porous Medium Construction and Instrumentation

The porous medium was constructed in a tank approximately 10 m long, 1.2 m tall, and 0.06 m inside width (Figure 1a). Each end of the porous medium consisted of a 20-cm section of pea gravel to provide constant-head boundaries for the system. The overall gradient and saturated-zone thickness were adjusted with a set of constant-head tanks that controlled the water level in the pea gravel. The water table was level with the top of the sand packing at the upgradient end of the tank. At the downgradient end it was 15.7 cm below the top of the packing, producing an overall gradient of approximately 0.016. This gradient, which is toward the high end of that found at field sites, provided a conservative evaluation: Density-induced sinking is less likely to be a significant component of transport at higher gradients. Deionized water was supplied to the upgradient constant-head tank. The gradient and resulting flow of approximately 3.3 L/h was maintained throughout each experiment and the periods between experiments. Between experiments, NaOCl was added to the deionized water supply to produce a one-pore-volume pulse of 100 ppm NaOCl solution, eliminating the potential for significant microbial growth within the tank.

A total of six different Tyler Mesh sieve size sands were used to pack the tank. Hydraulic conductivity of each sand was measured using a constant-head column according to ASTM D2434 [*American Society for Testing and Materials* (ASTM), 1994]. Additional tests using a two-dimensional tank verified the isotropy of the individual sands. The packing within the tank consisted of two zones: a homogeneous section of coarse

Table 1. Sand Parameters

	Tyler Mesh Size					
	#8	#16	#30	#50	#70	#110
K,[a] cm/h	4320	1550	540	133	48.6	15.1
d_{50}, mm	1.50	0.88	0.49	0.32	0.19	0.103
d_{60}/d_{10}	1.39	1.72	1.50	1.94	1.86	N/A

N/A, not available.
[a]From J. Mapa et al. (unpublished report for the U.S. Army Engineer Waterways Experiment Station, 1994).

sand (#8 sieve) in the upstream 1.1 m of the tank followed by an 8.1-m heterogeneous section (Figure 1a). The heterogeneous zone, created using five different sands, was included to produce transport results with statistical properties similar to heterogeneous field sites and was designed to support explicit representation in a numerical model. It approximated a log-normal distribution of K with a mean value of 4.18 ($\mu_{\ln K}$) and a variance of 1.22 ($\sigma^2_{\ln K}$), where K has units of cm/h. The lateral and vertical correlation scales were 50.8 and 5.08 cm, respectively. A continuous distribution with a negative exponential covariance was generated using a Fourier summation algorithm and then discretized into five categories. Each category was assigned a particular sieve size sand: #16, #30, #50, #70, or #110 (Table 1). *Chao et al*. [1996] verified that the discretized distribution matched the original continuous distribution in terms of $\mu_{\ln k}$, $\sigma^2_{\ln k}$, and the correlation structure. The homogeneous zone provided a region to inject the tracer and promote initial mixing as it exited the injection well, producing a relatively consistent vertical line source. The coarser sand, with a relatively high dispersivity, reduced the effect of microheterogeneities in the packing and the potential for variation from the injection well. Dye injections were used to verify that in the absence of severe density contrasts, the design allowed creation of relatively uniform line sources.

The sand was wet-packed in the tank to minimize consolidation and air entrapment. Each cell measured 25.4 cm long and 2.54 cm tall with overlapping ends (Figure 1b). Vertical interfaces were avoided to reduce the chance for preferential migration of nonaqueous phase liquids (NAPLs) used during other experiments. A total of 1280 cells were packed: 32 columns and 40 layers, producing 16 lateral and 20 vertical correlation scales. Packing of the tank followed a set procedure for each layer. First, using the constant-head tanks, the static water table was raised to approximately 4 cm above the most recently packed layer or above the base of the tank for the first layer. Depending on the layer's packing, up to 33 paddles, one on each edge of a sand cell, were mounted along the length of the tank, hanging down into the tank, providing separation between adjacent cells of different sands. Using a consistent length of drop tube and filling in the order from finest to coarsest, sands were dropped into their respective cells. After an individual or group of cells consisting of the same sand were filled, and prior to filling the neighboring coarser sands, the paddles were removed to allow the ends of the sand cell to slump so that the interfaces between dissimilar sands were not vertical (Figure 1b).

Hydraulic heads were monitored at 46 pressure ports (Figure 1a) using a pressure transducer and a hydraulic scanning valve that automatically switched between the ports. Data were collected and stored electronically. Measurement of a constant pressure source with each scan provided information for correcting any drift that occurred. Repeated scans ($N = 80$) indicated that the typical standard deviation of pressure head measurements was less than 0.08 cm of water. The effluent rate from the tank was periodically measured by collecting flow in a volumetric flask. The rate varied between 3.3 and 3.4 L/h for the different experiments, with a typical standard deviation of about 0.021 L/h for any individual experiment.

A 30-cm vertical line source, spanning about one third of the tank height, was used for the two-dimensional experiments. Longitudinal dispersion quickly increased the horizontal dimension of the resulting plume to several correlation lengths. The vertical source interval produced a plume that despite relatively small vertical dispersion, spanned multiple vertical correlation scales. The tracer plume arriving at the downgradient end of the tank had traversed multiple lateral correlation lengths and spanned multiple vertical correlation lengths, ensuring that the tracer plume shape reflected the overall transport characteristics of the hydraulic-conductivity distribution rather than a specific preferential flow path through the packed realization of the heterogeneous distribution.

An instantaneous injection would have caused significant disruption to the flow field. It was possible, however, to produce the line source over a relatively short period of time using a specially designed injection well described by *Barth* [1999]. The well consisted of a 0.635-cm-diameter stainless steel tubing injector with 24 evenly spaced outlets covered by #200 stainless steel mesh inserted into a fully screened PVC casing. Packers mounted on the stainless steel tubing ensured delivery of the tracer into the casing over the injection interval. Dye injections were performed in the tank to evaluate the injection well, but creation of a tracer plume with sufficient visual contrast to document its progress throughout the 10-m-long tank was outside of the objectives of this investigation.

Multicorrelation scale samplers (MC) were designed to provide a sample across approximately two vertical correlation scales. They require far less purge volume than a well installed from the top of the packing, thereby minimizing the potential impact of sampling on the flow field but still providing a sample from a physical interval, rather than a point sample. Each sampler consists of a vertical 10-cm-long perforated 0.32-cm-diameter piece of copper tubing wrapped with #200 stainless steel mesh. One end of the tubing is sealed, and the other is bent 90° and attached to a bulkhead compression fitting, allowing sampling through the tank wall. The sampler requires extraction of only about 1.5 mL to provide a 1-mL sample. A transect of six MC samplers, labeled MC7 (top) to MC12 (bottom) (Figure 1a), was used to measure the BTCs presented in this work. The samplers cover all but the top 10 cm and bottom 5 cm of the porous media. The saturated thickness above MC7 is of the order of a few centimeters due to the location of the sampler transect along the tank (Figure 1a) in relation to the sloping water table.

4.3. Tracer Injections

The results of four tracer tests are considered in this work (Table 2). The bromide (KBr) injections used about the same volume but different concentrations. The injection rate was approximately 3.0 L/h, just slightly less than the nominal tank effluent rate, to avoid flow field disruption. Decreasing concentration among experiments C5, C6, and C7 produced results with decreasing potential for density-induced sinking in each successive experiment. The final tracer test, D1, in which

Table 2. Tracer Injections

Experiment	Tank Effluent Rate, L/h	Injection Rate, L/h	Injection Period, hours	Concentration, M (KBr)	ρ_{rel}
C5	3.39	3.06	0.88	0.050	0.0039[a]
C6	3.36	3.04	0.92	0.010	0.0007[a]
C7	3.31	3.07	0.91	0.002	0.0001[b]
D1	3.30	3.01	0.93	N/A[c]	0.0000

[a]Measured directly.
[b]Based on linear extrapolation of direct measurements.
[c]Tritium was used as the tracer for experiment D1.

tritium (^{3}H; $\rho_{rel} = 0.0000$) was the tracer served as a control to verify the absence of density-induced sinking during C7. A repeat of experiment C7, not reported in this work, demonstrated close reproducibility. As indicated by application of the criteria proposed in this work and presented below, experiments C5, C6, and C7 demonstrate the three distinct outcomes possible for the experimental configuration: density-induced sinking throughout the tank, density-induced sinking only within the heterogeneous section, and no density-induced sinking.

4.4. Numerical Modeling of Flow

Although numerical simulation of density-induced transport was beyond the scope of this work, numerical simulations of the experiment were used to estimate the local hydraulic gradient in each sand cell to test the proposed criteria. The simulated local hydraulic gradients were calculated using the finite difference groundwater flow model MODFLOW [*McDonald and Harbaugh*, 1988]. The free surface in the tank was approximated using a stepped, no-flow boundary based on a calculated free surface. Comparison of flow predictions using the approximated boundary and a calculated free surface indicated little error from the approximation, as expected given the steady state flow field. The grid consisted of a single layer with 40 rows and 150 columns for a total of 6000 finite difference cells, each of which was approximately 2.5 cm tall and 6.4 cm long so that each 2.5-cm-tall, 25.4-cm-long sand cell was represented by four finite difference cells. The tapered ends of the sand cells shown in Figure 1b were not represented, but the resulting error is less than 1.5% [*Mehl*, 1998]. The upstream and downstream ends of the tank were represented as constant heads. Hydraulic-conductivity values for each sand that produced the best fit to measured heads and effluent from the tank were determined using MODFLOWP [*Hill*, 1992], and local hydraulic gradients were determined using the optimized values of hydraulic conductivity. The optimized values are close to the measured values of Table 1 but reproduced flow through the tank more accurately as discussed by *Barth* [1999] and *Barth et al*. [2000].

5. Results

This section presents the tracer-test data for the intermediate-scale experiments and the results of applying (8) to both these experiments and data from three field sites.

5.1. Intermediate-Scale Experimental Data

The BTC data collected from experiments C5, C6, and C7 at sampling ports MC7–MC12 are shown in Figure 2. The absence of density-induced sinking in C7 was verified by similarities in the BTC timing and shape between C7 and D1, in which tritium was used (Figure 3). Experiments C5 and C6 were clearly affected by density-induced sinking.

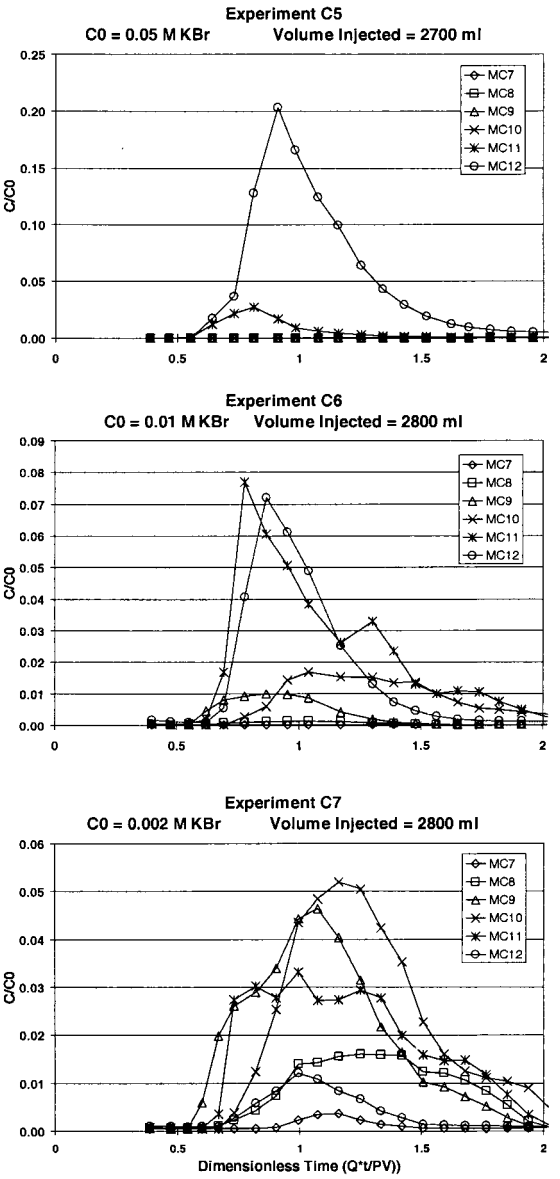

Figure 2. KBr breakthrough curves for all ports for experiments C5, C6, and C7. Density-induced sinking is more dramatic for higher C_0: Only ports MC11 and 12 respond when $C_0 = 0.05\ M$ (C5). For C6 ($C_0 = 0.01\ M$), the top two ports, MC7 and MC8, have no response, while for C7 ($C_0 = 0.002\ M$) all ports respond.

The cumulative mass as a function of depth at the sampler transect for experiments C5, C6, and C7 is shown in Figure 4. The curves graphically summarize the vertical distribution of solute as a function of decreasing C_0 (Table 2). Without density-induced sinking, the inflection point in each curve should occur at the vertical centroid of the injection line source, $Z_n = 0.52$, where Z_n is the depth normalized by the total height of the porous media. Density differences were most dramatic in experiment C5, in which a large portion of the injected mass (about 50%) flowed beneath the lowest sampler. In addition, the curve exhibits no inflection point. For C6, more than 75%

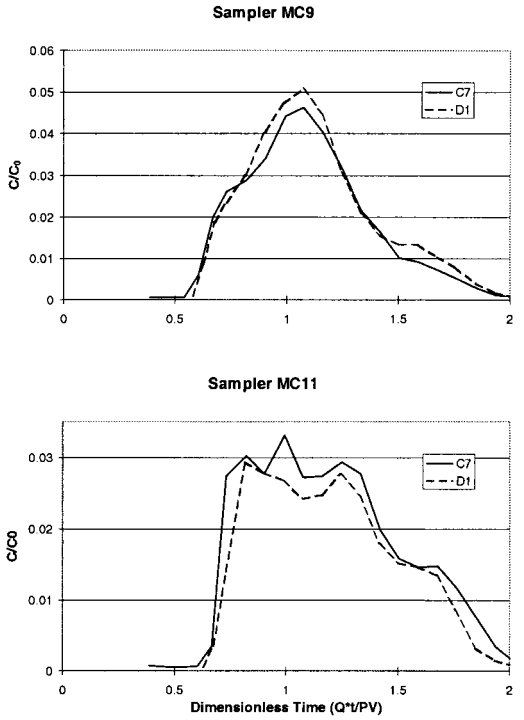

Figure 3. Absence of significant density-induced sinking during C7. Breakthrough curves from samplers MC7 and MC11 demonstrate similarity between the C7, bromide, and D1, tritium tests. The remaining ports exhibited similar agreement.

of the injected mass was accounted for and the inflection point is at about $Z_n = 0.65$. For C7 the mass accounted for exceeds 95%, and the vertical coordinate of the inflection point appears to have shifted toward the ideal value of $Z_n = 0.52$.

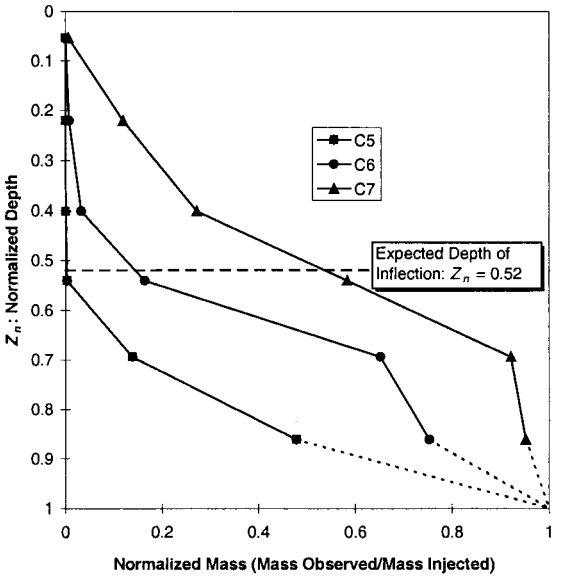

Figure 4. Normalized mass as a function of normalized depth. If there is no density-induced sinking, the expected depth of inflection is $Z_n = 0.52$. Experiment C5 contains no inflection point, while the first inflection point for C6 occurs significantly below $Z_n = 0.52$. For C7, the inflection point is close to $Z_n = 0.52$.

To evaluate whether the density-induced sinking was occurring in the homogeneous or heterogeneous portions of the tank, the simulated hydraulic gradients ($\Delta h/\Delta l$) for every sand cell and the ρ_{rel} of the injected concentration were used to produce a distribution of α_1' values for each experiment. These values are shown in Figure 5 and are summarized in Table 3. Figure 5 shows values for less than 6000 finite difference cells because the constant-head cells are excluded. The analysis indicates that density-induced sinking, evaluated using the gradients simulated within each finite difference cell, was significant ($\alpha_1' > 0.3$) in both the heterogeneous and homogeneous sections during experiment C5, in the homogeneous zone during experiment C6, and absent in C7. Evaluation of α_1' for the homogeneous section as a whole was, as expected, consistent with these results, indicating density-induced sinking for experiments C5 and C6 and not during C7. However, using the overall hydraulic gradient of the heterogeneous zone, α_1' fails to predict density-induced sinking for any of the intermediate-scale experiments (Figure 6). In contrast, using the overall gradient of the heterogeneous section and accounting for the variation in gradient, $\sigma_{j_1}^2$, (8) correctly predicts whether density-induced sinking occurs within the heterogeneous section for each of the experiments (Figure 6).

Evaluation of α_1' was based on the injected tracer concentration. Following injection, dispersion caused lateral and minor vertical stretching of the line-source plume, transforming it to a more classical elliptical shape as it moved away from the injector. Convergence and divergence of flow lines at the transition between the homogeneous and heterogeneous sections caused some distortion of the plume shape as it entered the heterogeneity. For the laboratory experiments presented in this work, however, C/C_0 values at the tracer plume centroid were approximately 0.9 as the plume entered the heterogeneous porous media, so analysis using the injected concentrations provided a good approximation.

5.2. Field Data

For the field data sets evaluated, $\sigma_{\ln K}^2$ is small (Table 4), reflecting very mild heterogeneity. Overall gradients typically cited for Borden, Cape Cod, and the Danish site are 0.0035–0.0054 [*Sudicky*, 1986], 0.0014–0.0018 [*LeBlanc et al.*, 1991], and about 0.0045 [*Jensen et al.*, 1993], respectively. The relatively small overall gradients and small $\sigma_{\ln K}^2$ mean that α_1' and α_2 are likely to be similar at these sites. However, as discussed above, these are the only field sites available for evaluating these criteria.

Cape Cod values of C/C_0 of the order of 0.9 were observed within the plume 13 days after injection [*LeBlanc et al.*, 1991], and at Borden, values of $C/C_0 > 0.95$ were observed after 43 days of transport [*Freyberg*, 1986]. At both sites, lateral migration during these respective periods was of the order of a single correlation scale, providing considerable opportunity for density-induced sinking to be a significant component of transport.

Evaluation of α_1' and α_2 for the field tracer tests at the Cape Cod and Danish sites indicates that they were subject to density-induced sinking (Figure 6 and Table 5). This is consistent with the observed plume migration [*LeBlanc and Celia*, 1991; *Jensen et al.*, 1993]. For the Borden site the reported range of α_2 results in statistics that straddle the critical value. For these examples, as a result of the mild degree of heterogeneity, the deviation of the local gradient from overall gradient is small enough that the α_1' and α_2 predictions are virtually identical

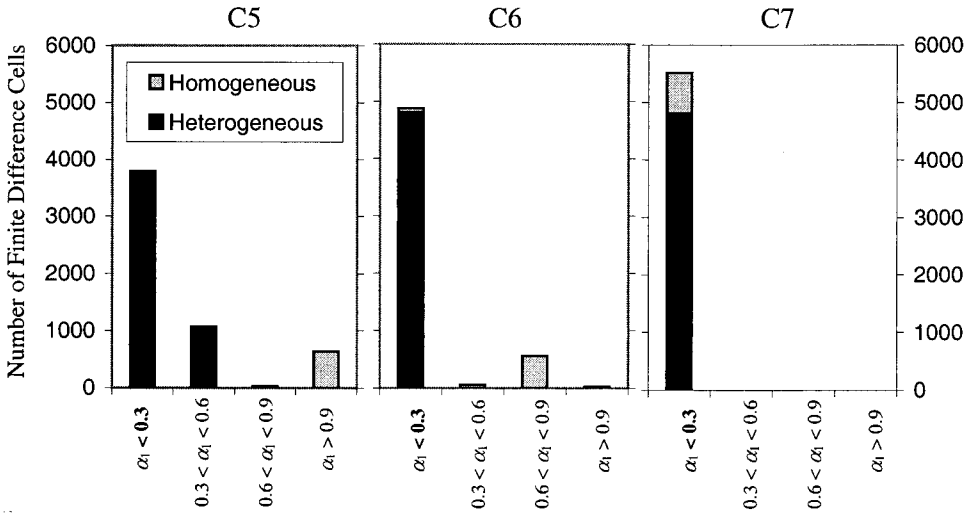

Figure 5. The α_1' values for, from left to right, C5, C6, and C7, by region of homogeneous or heterogeneous packing, calculated using simulated hydraulic gradients. In C5, some cells in the heterogeneous region have $\alpha_1' > 0.3$, indicating the potential for density-induced sinking in that region. In C6, all cells in the heterogeneous region have $\alpha_1' < 0.3$.

and predictions with either criterion are consistent with observations.

The similarity of α_1' and α_2 in these field cases prompts the question of when accounting for the local gradient variations would be important in typical field problems. This is discussed in the next section.

6. Discussion

Two remaining concerns of interest are (1) identifying when it is important to account for local variations in gradient, and (2) the severity of the restriction produced by the stationary-media assumption used to derive (5) and (6). These are addressed in this section.

6.1. Comparison of Results in Two and Three Dimensions

The value of the proposed dimensionless criterion, α_2, is sensitive to the correlation structure, represented using r, the variance of hydraulic conductivity, $\sigma^2_{\ln K}$, and the dimensionality of the flow system. For example, for Borden, Cape Cod, and the Danish site, (6) indicates that most local gradients would be within about $\pm 12\%$ of the overall gradient, and α_1' and α_2 are similar in value (Figure 6). In contrast, for the intermediate-scale experiments, limited to two dimensions and of a greater degree of heterogeneity, gradients varied by $\pm 71\%$ of the overall gradient, producing the much larger difference between α_1' and α_2 shown in Figure 6.

To compare the potential for density-induced sinking in two- and three-dimensional heterogeneous systems, criterion α_2 can be evaluated using (5) and (6), respectively. The variations in local gradient in two- and three-dimensional systems as a function of $\sigma^2_{\ln K}$ and r are shown in Figure 7. The adjustment to the overall gradient $(2\sigma_j)$ normalized by the overall gradient (J) is plotted as a function of $\sigma^2_{\ln K}$ for a variety of r values for two- and three-dimensional systems. As $(2\sigma_j)/J$ approaches 1.0, the variation in local gradient approaches the magnitude of the overall gradient. In general, three-dimensional systems are not

Table 3. Location and Occurrence of Significant Density-Induced Sinking as Determined by Simulated Local Gradients

Experiment	Homogeneous Zone	Heterogeneous Zone
C5	yes	yes
C6	yes	no
C7	no	no

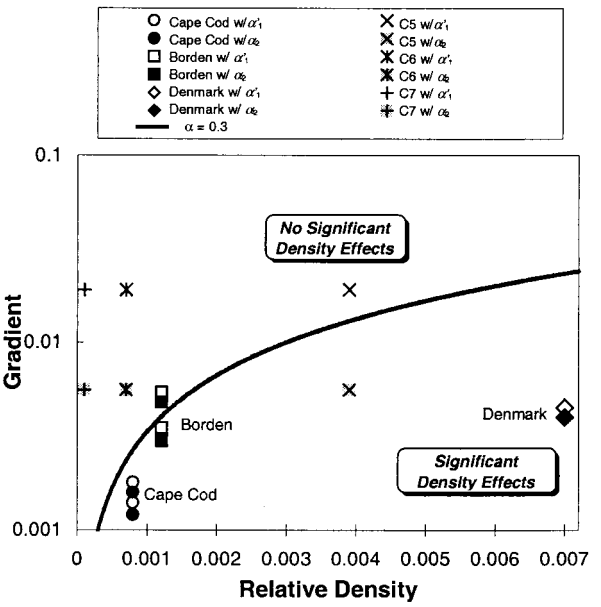

Figure 6. Predictions of density-induced sinking for the published field tracer tests and for experiments C5, C6, and C7 within the heterogeneous section using the original (α_1') and the proposed (α_2) criteria. Multiple values for the field sites reflect the approximate range of overall gradient and the range of reported hydraulic conductivity variances for the Danish site and for Borden and Cape Cod, respectively.

Table 4. Comparison of Laboratory and Field Site Values of $\Delta\rho/\rho_0$

Experiment or Field Site	Overall Gradient	Typical Local-Gradient Range	$\Delta\rho/\rho_0$	Variance of ln K
Borden	0.0035–0.0054[a]	0.0031–0.0060	0.0012[b]	0.24–0.37[c]
Cape Cod	0.0014–0.0018[d]	0.0012–0.0020	0.0008[e]	0.24[f]
Denmark	0.0045–0.0050[g]	0.0040–0.0060	0.0070[g]	0.37[g]
C5	0.0160	0.0046–0.0274	0.0039	1.22
C6	0.0160	0.0046–0.0274	0.0007	1.22
C7	0.0161	0.0047–0.0274	0.0001	1.22

[a]*Sudicky* [1986].
[b]*Mackay et al*. [1986].
[c]*Woodbury and Sudicky* [1991].
[d]*LeBlanc et al*. [1991].
[e]*LeBlanc and Celia* [1991].
[f]*Hess et al*. [1992].
[g]*Jensen et al*. [1993].

as sensitive to $\sigma^2_{\ln K}$ and r as two-dimensional systems. For the same values of $\sigma^2_{\ln K}$ and r, the variation in local gradient is more pronounced for two dimensions. A third dimension provides additional alternative flow paths, reducing the probability of flow forced through high-contrast transitions in hydraulic conductivity, thereby reducing the variability in local gradients. As $\sigma^2_{\ln K}$ increases, the potential for density-induced sinking is greater due to the increasing probability that some local gradients are very small. On the other hand, as r increases, the porous media becomes dominated by layering parallel to the overall gradient, J, and the local gradient variation is reduced. In highly stratified systems, with flow parallel to the stratification, variability of the local gradient becomes insignificant as $r \rightarrow \infty$ and α_2 reduces to α_1'.

6.2. Applicability of Criterion to Nonstationary Media

Variations of the approach presented in this work could produce criteria for non-Gaussian, or even nonstationary, heterogeneity. In the absence of detailed information about subsurface heterogeneity, or for sites that clearly violate second-order stationarity, the approach presented provides insight into the potential for density-induced sinking. Even a simple accounting, based on basic geologic characteristics at a site, could be used to adjust or replace the overall gradient term used in (8), providing a more realistic assessment of the potential for density-induced sinking.

7. Conclusions

This paper presents a new dimensionless criterion for predicting density-induced sinking in tracer tests in heterogeneous systems and evaluates its viability using a series of heterogeneous, intermediate-scale experiments and three well-documented field-scale tracer experiments. An existing dimensionless parameter reported in the literature for homogeneous media is modified to incorporate statistics of the hydraulic conductivity distribution and the overall gradient. The value of the proposed criterion (α_2) is interpreted in terms of a critical value determined by *Oostrom et al*. [1992a] to indicate the onset of instabilities but is used here to indicate density-induced sinking by any mechanism. Values greater than the critical value are taken to indicate that density-induced sinking occurs, and values less than the critical value indicate no significant density effects.

The modified parameter, α_2, correctly predicted the occurrence or absence of density-induced sinking within the heterogeneous zone for each intermediate-scale experiment and produced results in agreement with observations from the three well-documented field experiments. Evaluating α_2 for a range of hypothetical hydraulic conductivity distributions demonstrated that the potential for density-induced sinking increases with increasing $\sigma^2_{\ln k}$, decreases with increases in the correlation length ratio, and, all else being equal, is greater in two-dimensional than three-dimensional heterogeneous fields. Even in three-dimensional systems, however, accounting for heterogeneity could indicate that the density of an injected tracer needs to be much smaller than would be indicated based

Table 5. Values of Dimensionless Parameters α_1' and α_2

Case	α_1'	α_2
C5 (heterogeneous zone): $\sigma^2_{\ln K} = 1.22$	0.25	(0.70)
C6 (heterogeneous zone): $\sigma^2_{\ln K} = 1.22$	0.04	0.13
C7 (heterogeneous zone): $\sigma^2_{\ln K} = 1.22$	0.01	0.02
Borden: $J_1 = 0.0054$, $\rho_{rel} = 0.0012$, $\sigma^2_{\ln K} = 0.24$	0.22	0.25
Borden: $J_1 = 0.0035$, $\rho_{rel} = 0.0012$, $\sigma^2_{\ln K} = 0.24$	(0.35)	(0.39)
Cape Cod: $J_1 = 0.0018$, $\rho_{rel} = 0.0008$, $\sigma^2_{\ln K} = 0.2$	(0.44)	(0.50)
Cape Cod: $J_1 = 0.0014$, $\rho_{rel} = 0.0008$, $\sigma^2_{\ln K} = 0.2$	(0.57)	(0.65)
Denmark: $J_1 = 0.0050$, $\rho_{rel} = 0.007$, $\sigma^2_{\ln K} = 0.37$	(1.40)	(1.62)
Denmark: $J_1 = 0.0045$, $\rho_{rel} = 0.007$, $\sigma^2_{\ln K} = 0.37$	(1.56)	(1.80)

Values in parentheses exceed the critical value.

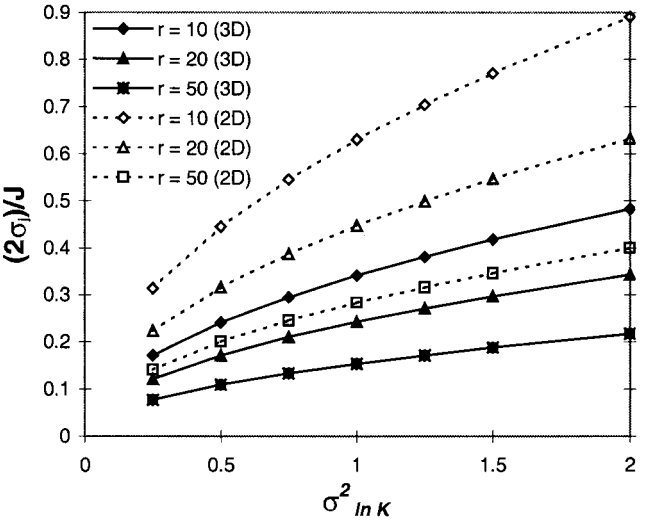

Figure 7. Two standard deviations of the local gradient ($2\sigma_j$) normalized by the overall gradient (J) as a function of the variance of ln K ($\sigma^2_{\ln K}$) and r, the ratio of longitudinal to transverse correlation scales ($r = \lambda_1/\lambda_2$).

on an analysis assuming homogeneity. The criterion relies on a simplified interpretation of the physical system, focusing only on the overall and local hydraulic gradients, and the ratio of tracer to ambient fluid density. This work indicates that any criterion in which the hydraulic gradient is used, or which can be rearranged to include the hydraulic gradient, can be improved by accounting for local gradient variations using the modification presented here.

Acknowledgments. This research was funded by the U.S. EPA Great Plains–Hazardous Substance Research Center, the U.S. Army Research Office, Terrestrial Division, and by the U.S. Geological Survey. Comments from Hillel Rubin, Li Zheng, an anonymous reviewer, and the associate editor were greatly appreciated and very helpful in improving the manuscript.

References

Adams, E. E., and L. W. Gelhar, Field study of dispersion in a heterogeneous aquifer, 2, Spatial moments analysis, *Water Resour. Res*., *28*(12), 3293–3307, 1992.

American Society for Testing and Materials, *1994 Annual Book of ASTM Standards*, vol. 4.08, West Conshohocken, Pa., 1994.

Bachmat, Y., and D. E. Elrick, Hydrodynamic instability of miscible fluids in a vertical porous column, *Water Resour. Res*., *6*(1), 156–171, 1970.

Barth, G. R., Intermediate-scale tracer tests in heterogeneous porous media: Investigation of density, predictability and characterization of NAPL entrapment, Ph.D. dissertation, 320 pp., Dep. of Civ. Eng., Univ. of Colo., Boulder, 1999.

Barth, G. R., M. C. Hill, T. H. Illangaskare, and H. Rajaram, Predictive modeling of flow in two-dimensional intermediate-scale heterogeneous porous media, in *Calibration and Reliability in Groundwater Modeling*, *IAHS Publ*., *265*, 265–271, 2000.

Boggs, J. M., S. C. Young, L. M. Beard, L. W. Gelhar, K. R. Rehfeldt, and E. E. Adams, Field study of dispersion in a heterogeneous aquifer, 1, Overview and site description, *Water Resour. Res*., *28*(12), 3281–3291, 1992.

Chao, H. C., H. Rajaram, and T. H. Illangasekare, Experimental and computational investigation of radial flow tracer tests in heterogeneous formations, *Eos Trans. AGU*, *77*(46), Fall Meet. Suppl., F275, 1996.

Fan, Y., and R. Kahawita, A numerical study of variable density flow and mixing in porous media, *Water Resour. Res*., *30*(10), 2707–2716, 1994.

Freyberg, D. L., A natural gradient experiment on solute transport in a sand aquifer, 2, Spatial moments and the advection and dispersion of nonreactive tracers, *Water Resour. Res*., *22*(13), 2031–2046, 1986.

Garabedian, S. P., D. R. LeBlanc, L. W. Gelhar, and M. A. Celia, Large-scale natural gradient tracer test in sand and gravel, Cape Cod, Massachusetts, 2, Analysis of spatial moments for a nonreactive tracer, *Water Resour. Res*., *27*(5), 911–924, 1991.

Gelhar, L. W., *Stochastic Subsurface Hydrology*, Prentice-Hall, Englewood Cliffs, N. J., 1993.

Hess, K. M., S. H. Wolf, and M. A. Celia, Large-scale natural gradient tracer test in sand and gravel, Cape Cod, Massachusetts, 3, Hydraulic conductivity variability and calculated macrodispersivities, *Water Resour. Res*., *28*(8), 2011–2027, 1992.

Hill, M. C., A computer program (MODFLOWP) for estimating parameters of a transient, three-dimensional groundwater flow model using nonlinear regression, *U.S. Geol. Surv. Open File Rep*., *91-484*, 358 pp., 1992.

Humphrey, M. D., Experimental design of physical aquifer models for evaluation of groundwater remediation strategies, M.S. thesis, Oreg. State Univ., Corvallis, 1992.

Istok, J. D., and M. D. Humphrey, Laboratory investigation of buoyancy-induced flow (plume sinking) during two-well tracer tests, *Ground Water*, *33*(4), 597–604, 1995.

Jensen, K. H., K. Bitsch, and P. L. Bjerg, Large-scale dispersion experiments in a sandy aquifer in Denmark: Observed tracer movements and numerical analyses, *Water Resour. Res*., *29*(3), 673–696, 1993.

LeBlanc, D. R., and M. A. Celia, Density-induced downward movement of solutes during a natural-gradient tracer test, Cape Cod, Massachusetts, U.S. Geological Survey Toxic Substances Hydrology Program, Monterey, California, *U.S. Geol. Surv. Water Resour. Invest. Rep*., *91-4034*, 10–14, 1991.

LeBlanc, D. R., S. P. Garabedian, K. M. Hess, L. W. Gelhar, R. D. Quadri, K. G. Stollenwerk, and W. W. Wood, Large-scale natural gradient tracer test in sand and gravel, Cape Cod, Massachusetts, 1, Experimental design and observed tracer movement, *Water Resour. Res*., *27*(5), 895–910, 1991.

Libicki, J., Effects on the disposal of coal waste and ashes in open pits, *Rep. EPA-600/7-78-067*, Ind. Environ. Res. Lab., U.S. Environ. Prot. Agency, Cincinnati, Ohio, 1978.

List, E. J., The stability and mixing of a density-stratified horizontal flow in a saturated medium, *Rep. KH-R-11*, Calif. Inst. of Technol., Pasadena, 1965.

Liu, H. H., A physical and numerical model study on variable density flow and mixing in porous media, Ph.D. dissertation, Dep. of Agron. and Soils, Auburn Univ., Auburn, Ala., 1995.

Liu, H. H., and J. H. Dane, A numerical study on gravitational instabilities of dense aqueous phase plumes in three-dimensional porous media, *J. Hydrol*., *194*, 126–142, 1997.

Mackay, D. M., D. L. Freyberg, P. V. Roberts, and J. A. Cherry, A natural gradient experiment on solute transport in a sand aquifer, 1, Approach and overview of plume movement, *Water Resour. Res*., *22*(13), 2017–2029, 1986.

McDonald, M. G., and A. W. Harbaugh, A modular three-dimensional finite-difference groundwater flow model, *U.S. Geol. Surv. Tech. Water Resour. Invest*., *Book 6*, chap. A1, 586 pp., 1988.

Mehl, S., Experimental and numerical investigations of intermediate-scale experiments, M.S. thesis, Univ. of Colo., Boulder, 1998.

Moltyaner, G. L., and C. A. Wills, Local- and plume-scale dispersion in the Twin Lakes 40- and 260-m natural-gradient tracer tests, *Water Resour. Res*., *27*(8), 2007–2026, 1991.

Oostrom, M., J. S. Hayworth, J. H. Dane, and O. Guven, Behavior of dense aqueous phase leachate plumes in homogeneous porous media, *Water Resour. Res*., *28*(8), 2123–2134, 1992a.

Oostrom, M., J. H. Dane, O. Guven, and J. S. Hayworth, Experimental investigation of dense solute plumes in an unconfined aquifer model, *Water Resour. Res*., *28*(9), 2315–2326, 1992b.

Oostrom, M., A. Leijnse, J. H. Dane, and O. Guven, Simulation of variable density, aqueous phase contaminant plumes with the METROPOL code, in *Agronomy Abstracts*, p. 225, Soil Sci. Soc. of Am., Madison, Wisc., 1992c.

Paschke, N. W., and J. A. Hoopes, Buoyant contaminant plumes in groundwater, *Water Resour. Res*., *20*(9), 1183–1192, 1984.

Schincariol, R. A., and F. W. Schwartz, An experimental investigation of variable density flow and mixing in homogeneous and heterogeneous media, *Water Resour. Res*., *26*(10), 2317–2329, 1990.

Schincariol, R. A., F. W. Schwartz, and C. A. Mendoza, On the generation of instability in variable density flow, *Water Resour. Res*., *30*(4), 913–927, 1994.

Sudicky, E. A., A natural gradient experiment on solute transport in a sand aquifer: Spatial variability of hydraulic conductivity and its role in the dispersion process, *Water Resour. Res*., *22*(13), 2069–2082, 1986.

Woodbury, A. D., and E. A. Sudicky, The geostatistical characterization of the Borden aquifer, *Water Resour. Res*., *27*(4), 533–546, 1991.

Wooding, R. A., The stability of a viscous liquid in a vertical tube containing porous material, *Proc. R. Soc. London*, *Ser. A*, *252*, 120–134, 1959.

Wooding, R. A., Free convection of fluid in a vertical tube filled with porous material, *J. Fluid Mech*., *13*, 129–144, 1962.

Wooding, R. A., Growth of fingers at an unstable diffusing interface in a porous medium or Hele-Shaw cell, *J. Fluid Mech*., *39*, 477–495, 1969.

Yeh, T.-C. J., J. Mas-Pla, T. M. Williams, and J. F. McCarthy, Observation and three-dimensional simulation of chloride plumes in a sandy aquifer under forced-gradient conditions, *Water Resour. Res*., *31*(9), 2141–2157, 1995.

G. R. Barth and M. C. Hill, U.S. Geological Survey, 3215 Marine Street, Boulder, CO 80303-1066. (barthg@bechtel.colorado.edu)

T. H. Illangasekare, Division of Environmental Sciences and Engineering, Colorado School of Mines, Golden, CO 80401-1887.

H. Rajaram, Department of Civil and Environmental Engineering, University of Colorado, Boulder, CO 80309-0428.

(Received March 6, 2000; revised August 2, 2000;
accepted September 12, 2000.)